

THE EFFECT OF AN EXTERNAL ELECTROMAGNETIC FIELD ON ORTHOGONAL COUPLED MICROSTRIP TRANSMISSION LINES

M. Baqerian, A. Arshadi, and A. Cheldavi

College of Electrical Engineering
Iran University of Science and Technology
Tehran, Narmak 16846, Iran

Abstract—The response of a two-layer structure of orthogonal coupled microstrip transmission lines illuminated by an external electromagnetic field has been studied. A simple model for the crosstalk region using lumped capacitance and inductance elements is used. The effect of the external EM field on the microstrip lines will be obtained using the method taking into account the EM field in order to reach transmission line equations along the lines. The model is finally validated using the full wave analysis simulator, HFSS. Voltage and current along the lines obtained by the present method are in good agreement with the results of the full wave analysis (HFSS). The proposed model has been used for voltage and current in terminal ports up to 10 GHz. This method can be developed simply for multilayer structures.

1. INTRODUCTION

A large number of papers have been devoted to the analysis of various types of planar transmission lines with multilayer dielectric media. Among them, the quasi-static analysis gives reasonable results with less computational effort. Recent advances in microwave solid-state devices have stimulated interest in the integration of microwave circuits. Multilayered coupled-microstrip lines are being widely used at present in designing microwave integrated circuits.

A transmission line theory has been introduced to study the effect of electromagnetic field on a microstrip in the dielectric substrate [1]. A new model for crossed orthogonal lines in [2–5] has utilized lumped elements taking into account the coupling in the crosstalk region.

Corresponding author: A. Arshadi (a.arshadi@gmail.com).

A new and simple lumped model was introduced for two crossed orthogonal coupled strip lines in [2]. This idea was generalized in [3] for an arbitrary number of orthogonal interconnects in an arbitrary number of layers. There are a lot of classical models to analyze simple and parallel coupled multiconductor lines on the same layer or on different layers [5–10]. Different parameters of coupled microstrip lines have been studied [20–25] and many electronic devices using coupled MTLs have been fabricated with IC technology [26–38]. Multilayer printed circuit boards are used in several applications to reduce the coupling phenomenon between adjacent layers. Orthogonal strip lines decrease the coupling effect between the lines in two different layers. The problem of crossed lines in the time and frequency domains has been considered in [11, 12]. Static analysis of crossed planar multiconductor structure has been examined in [11] using the method of lines. Also, [12] analyzed coupled strip lines with crossed strips in the frequency domain.

In this paper, a rigorous electromagnetic theory for quasi-static fields [1] and a model of the cross talk region [2, 3] have been used in order to model the effect of an external electromagnetic field on orthogonal microstrip lines in a two-layer structure. The entire coupling phenomenon between the lines is assumed to be concentrated in the crosstalk region located in the center of both lines.

Lumped elements of capacitances and inductances are used to simulate the coupling in the cross talk region. This model simulates the behavior of an orthogonal coupled microstrip transmission line in two different layers excited by external fields with a great accuracy.

The voltage and current of the equivalent circuit are calculated along the length of the lines and compared with those obtained from full wave analysis (HFSS). The results show good agreement up to 3 GHz.

2. THE STRUCTURE AND ITS EQUIVALENT MODEL

Figure 1 shows the structure considered in this work, where two orthogonal microstrip lines of length L_x and L_y are illuminated by a time harmonic uniform plane wave. The upper strip with width w_{up} and height d is directed along the x -axis on the boundary of the dielectric and free space, and the lower strip with width w_{down} and height $d - h$ is directed along the y -axis in the dielectric media. The width and height of these lines are designed for a $50\ \Omega$ characteristic impedance. The ground plane and the strips are perfect conductors and the dielectric is a lossless substrate with the permittivity $\epsilon_r \epsilon_0$.

In the quasi-TEM approximation, for each line, the electric field

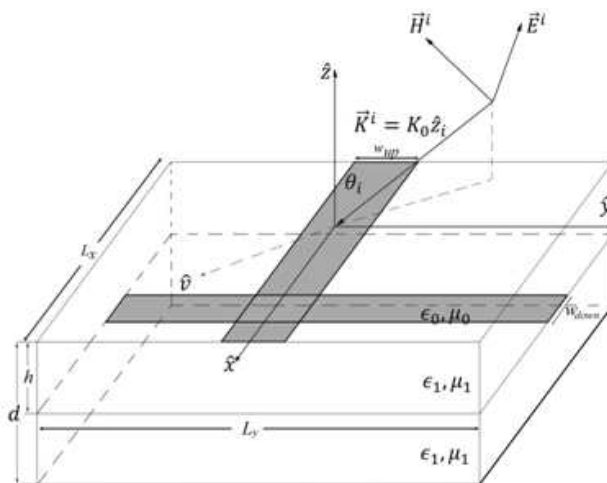


Figure 1. Two orthogonal microstrip lines illuminated by an external EM wave.

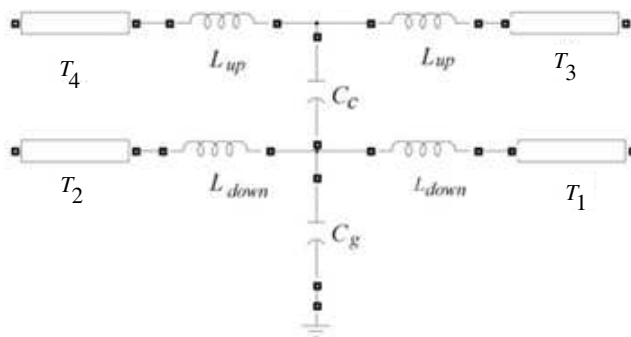


Figure 2. Model of the orthogonal lines including the crosstalk region.

lines are tied vertically to the ground planes and magnetic field lines in this mode are closed around the strips. In the crosstalk region, most of the electric field lines of the upper strip are closed to the down strips. Fig. 2 shows the model that has been used for this region. The entire coupling phenomenon in this model is assumed to be in the crosstalk region in the center of both the strip lines. So we have 4 uncoupled sections of transmission lines and a network of lumped elements representing the cross talk region, as shown in Fig. 2. T_1 and T_2 represent the lower strip and T_3 and T_4 represent the upper strip.

There are many formulas for the capacitance and inductance per unit length of ideal microstrip and strip lines [13–19]. The coupling between two layers has been simulated with C_c in this model. So, the mutual capacitance of the cross talk region is obtained as [13, 14]:

$$C_c = \frac{w_{down}}{h} \left(\epsilon_r - \frac{\epsilon_r - \epsilon_{eff}}{1 + G \left(\frac{f}{fp} \right)^2} \right) \left(w_{down} + \frac{W_{eff} - w_{down}}{1 + \left(\frac{f}{fp} \right)^2} \right) \quad (1)$$

where

$$G = 0.6 + 0.009Z_w \quad (2)$$

$$fp = \frac{Z_w}{2\mu_0 d} \quad (3)$$

$$W_{eff} = \frac{d\eta}{Z_w \sqrt{\epsilon_{eff}}} \quad (4)$$

$$\eta = \sqrt{\frac{\mu_0}{\epsilon_0}} \quad (5)$$

and

$$\epsilon_{eff} = \frac{1}{2} \left[\epsilon_r + 1 + (\epsilon_r - 1) \left(1 + 10 \frac{d}{w_{down}} \right)^{-0.5} \right] \quad (6)$$

In (2) Z_w is characteristic impedance.

Some of the E -field lines of the lower strip are closed to the ground plane. This effect is modeled by the capacitance $C_g \left(\frac{F}{m} \right)$. For a microstrip line structure, the capacitance per unit length can be obtained from [15]:

$$C_g = \begin{cases} 4\epsilon_r \epsilon_0 \left(\frac{w_{down}}{d-h} + \frac{2}{\pi} \text{Ln}2 \right) & \frac{w_{down}}{d-h} > 3 \\ 2\pi \epsilon_r \epsilon_0 \left[\text{Ln} \left(\frac{16(d-h)}{\pi w_{down}} + \frac{\pi^2}{48} \frac{w_{down}^2}{4(d-h)^2} \right) \right]^{-1} & \frac{w_{down}}{d-h} < 3 \end{cases} \quad (7)$$

Inductances in this model represent the length of crosstalk region. Assuming the current distribution of the strips to be uniform, one has [19]:

$$L = \frac{\mu_0 \ell}{2\pi} \left[\text{Ln}(u + \sqrt{u^2 + 1}) + \frac{u^2}{3} + \frac{1}{3u} + u \text{Ln} \left(\frac{1}{u} + \sqrt{\frac{1}{u^2} + 1} \right) - \frac{1}{3u} (u^2 + 1)^{\frac{3}{2}} \right] \quad (8)$$

when $u = l/w$, $u_{down} = \frac{w_{up}}{2w_{down}}$ and $u_{up} = \frac{w_{down}}{2w_{up}}$.

3. TRANSMISSION LINE EQUATIONS

Voltage and current induced in the upper and lower strips will be studied using a distributed source transmission line model [1]. We consider the equation $\nabla \times E = -j\omega\mu H$ and integrate over the area enclosed by the path shown in Fig. 3. Using Stokes' theorem we have

$$-\frac{d}{dy} \int_{-d}^{-h} E(0, y, z) \cdot \hat{z} dz = j\omega\mu \int_{-d}^{-h} H(0, y, z) \cdot \hat{x} dz \quad (9)$$

Next the quantity $\nabla \cdot (J + j\omega\epsilon E) = 0$ is considered. It is integrated over the volume shown in Fig. 4 which encompasses the strip and the divergence theorem is applied:

$$\begin{aligned} & \frac{d}{dy} \int_{-\frac{w_{down}^2}{2}}^{\frac{w_{down}}{2}} J_s(x, y) \cdot \hat{y} dx \\ &= -j\omega\epsilon_1 \int_{-\frac{w_{down}^2}{2}}^{\frac{w_{down}}{2}} [E(x, y, -h^+) - E(x, y, -h^-)] \cdot \hat{z} dx \end{aligned} \quad (10)$$

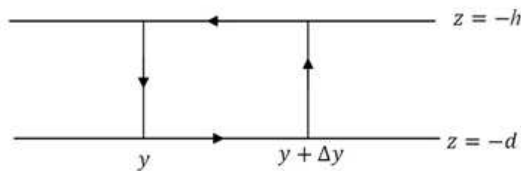


Figure 3. Contour of integration in the y - z plane.

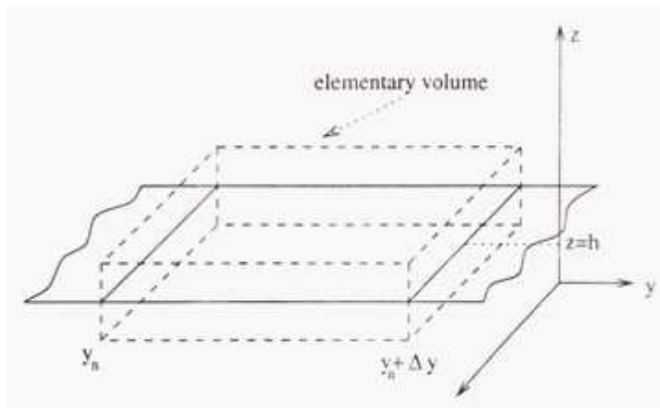


Figure 4. Volume chosen for integrating the quantity equation.

Defining following quantities:

induced voltage

$$V(y) = - \int_{-d}^{-h} E(0, y, z) \cdot \hat{z} dz \quad (11)$$

induced current

$$I(y) = \int_{-\frac{w_{down}^2}{2}}^{\frac{w_{down}^2}{2}} J_s(x, y) \cdot \hat{y} dx \quad (12)$$

electric charge per unit length

$$Q(y) = \int_{-\frac{w_{down}^2}{2}}^{\frac{w_{down}^2}{2}} [E(x, y, -h^+) - E(x, y, -h^-)] \cdot \hat{z} dx \quad (13)$$

and magnetic flux per unit length

$$\phi(y) = -\mu_0 \int_{-d}^{-h} H(0, y, z) \cdot \hat{x} dz \quad (14)$$

we will have

$$\begin{cases} \frac{d}{dy} V(y) = -j\omega\phi(y) \\ \frac{d}{dy} I(y) = -j\omega Q(y) \end{cases} \quad (15)$$

Based on the solving method of [1] we separate the contribution of the external field from that of the scattered field. The total field is decomposed to sum of a “primary” and “secondary” field with superscripts p and s , respectively:

$$\begin{cases} E = E^p + E^s \\ H = H^p + H^s \end{cases} \quad (16)$$

The “primary” field is defined as the field exited by the incident electromagnetic field in the presence of the ground plane and the dielectric substrate, and in the absence of the metal strip. The “secondary” field is the field scattered by metal strip when exited by the “primary” field in the presence of the ground plane and the dielectric substrate. From (15) and (16) we have

$$\begin{cases} \frac{d}{dy} V(y) = -j\omega\phi^s(y) - j\omega\phi^p(y) \\ \frac{d}{dy} I(y) = -j\omega Q(y) \end{cases} \quad (17)$$

where

$$\phi^i(y) = -\mu_0 \int_{-d}^{-h} H^i(0, y, z) \cdot \hat{x} dz; \quad i = p, s \quad (18)$$

Now with the assumption that all of the fields are quasi TEM, we can define a per unit length inductance L and a per unit length capacitance

C:

$$L = \frac{\phi^s}{I} = - \frac{\int_{-d}^{-h} H^s(0, y, z) \cdot \hat{x} dz}{\int_{-\frac{w_{down}^2}{2}}^{\frac{w_{down}^2}{2}} J_s(x, y) \cdot \hat{y} dx} \quad (19)$$

$$C = \frac{Q}{V^s} = \frac{\int_{-\frac{w_{down}^2}{2}}^{\frac{w_{down}^2}{2}} [E^s(x, y, -h^+) - E^s(x, y, -h^-)] \cdot \hat{z} dx}{\int_{-d}^{-h} E^s(0, y, z) \cdot \hat{z} dz} \quad (20)$$

It is clear that L and C are independent from the incident wave and determined only by the physical structure. We can rewrite (17) using these definitions

$$\begin{cases} \frac{d}{dy} V(y) = -j\omega LI(y) - j\omega\phi^p(y) \\ \frac{d}{dy} I(y) = -j\omega CV(y) + j\omega CV^p(y) \end{cases} \quad (21)$$

From (21) the transmission line equations describing this structure can be written in the form

$$\begin{cases} \frac{d}{dy} V(y) + j\omega LI(y) = V_F(y) \\ \frac{d}{dy} I(y) + j\omega CV(y) = I_F(y) \end{cases} \quad (22)$$

which $V_F(y) = -i\omega\phi^p(y)$ and $I_F(y) = j\omega CV^p(y)$. The structure is illuminated by a uniform plane wave propagating in the \hat{z}_l direction that forms an angle θ_i with the z axis (Fig. 1):

$$\vec{E}^i = \vec{E}_0 e^{-j\vec{K}^i \cdot \vec{r}} \quad (23)$$

$$\vec{H}^i = \sqrt{\frac{\epsilon_0}{\mu_0}} \hat{z}_i \times \vec{E}_0 e^{-j\vec{K}^i \cdot \vec{r}} \quad (24)$$

$$\vec{K}^i = K_0 \hat{z}_i = \omega \sqrt{\mu_0 \epsilon_0} \hat{z}_i \quad (25)$$

$$\hat{z}_i \cdot \hat{z} = -\cos \theta_i \quad (26)$$

The propagation vector \vec{K}^i can be decomposed into transverse and axial components with respect to the \hat{z} direction

$$\vec{K} = \vec{K}_t + K_z \hat{z} = K_t \hat{v} + K_z \hat{z} \quad (27)$$

$$\hat{u} \times \hat{v} = \hat{z} \quad (28)$$

In this new coordinate system the plane of incidence is the v - z plane. The incident plane wave is decomposed into the sum of TE (E normal to the plane of incidence and directed as \hat{u}) and TM (E lying in the plane of incidence) waves.

Based on transmission line theory, the current and the voltage along the length of a line oriented in the y axis will be written in the form of two coupled differential equations:

$$\begin{cases} \frac{dV}{dy} + jZK_z I = 0 \\ \frac{dI}{dy} + j\frac{K_z}{Z} V = 0 \end{cases} \quad (29)$$

If we use the transmission line model to analyze our structure, by a comparison between (29) and Maxwell equation ($\nabla \times E = -j\omega\mu H$, $\nabla \times H = j\omega\epsilon E$) for TE and TM mode, we will have

$$Z_{wj}^{TM} = \frac{K_{zj}}{w\epsilon_j}, \quad j = 1, 2 \quad (30)$$

$$Z_{wj}^{TE} = \frac{\omega\mu_0}{K_{zj}}, \quad j = 1, 2 \quad (31)$$

and the propagation constants are:

$$K_{zj} = K_0 \sqrt{(\epsilon_{rj} - 1) + (\hat{\mathbf{z}}_i \cdot \hat{\mathbf{z}})^2}, \quad j = 1, 2 \quad (32)$$

In (30)–(32) the index $j = 1$ refers to the dielectric substrate and $j = 2$ to the free space; ϵ_{r1} is the relative permittivity of the substrate and ϵ_{r2} that of free space. Finally for the lower strip we obtain

$$I_F(y) = j\omega CV^p(y) = j2K_t \frac{C \sin K_{z1}(d-h)}{\epsilon_1 K_{z1}} e^{-jK_y y} \times \frac{E_0 \cdot \hat{\mathbf{v}}}{jZ_{w1}^{TM} \sin K_{z1}d + Z_{w2}^{TM} \cos K_{z1}d} \quad (33)$$

$$V_F(y) = -j\omega\phi^p(y) = j2\omega\mu_0 \frac{\sin K_{z1}(d-h)}{K_{z1}} e^{-jK_y y} \times \left[\frac{E_0 \cdot \hat{\mathbf{v}} \hat{\mathbf{u}} \cdot \hat{\mathbf{x}}}{jZ_{w1}^{TM} \sin K_{z1}d + Z_{w2}^{TM} \cos K_{z1}d} + \frac{E_0 \cdot \hat{\mathbf{u}} \hat{\mathbf{v}} \cdot \hat{\mathbf{x}}}{jZ_{w1}^{TM} \sin K_{z1}d + Z_{w2}^{TE} \cos K_{z1}d} \right] \quad (34)$$

There are relations like those mentioned above for the strip on the boundary of the substrate and free space. There is a subtle modification in the equations describing the voltage and the current in the upper strip. First of all the change in the height and width of the upper strip in comparison with those of the lower strip should be considered, and then it is very important to do replacements of $x \rightarrow y$ and $y \rightarrow -x$ for the upper strip because of the change in rectangular coordinates.

For each line we have a system of equations with 4 unknowns. In order to solve these differential equations and determine the voltage

and current along the length of the lines, boundary conditions should be written at $x = 0^\pm$ and $x = \pm\ell/2$ for the upper strip and $y = 0^\pm$ and $y = \pm\ell/2$ for the lower strip. Boundary conditions at $\pm\ell/2$ are related to the termination ports and at 0^\pm to the network model of the crosstalk region. Now we have the following 8 boundary conditions and our equations are solvable:

$$V_1\left(\frac{\ell}{2}\right) = Z_w I_1\left(\frac{\ell}{2}\right) \quad (35)$$

$$V_2\left(-\frac{\ell}{2}\right) = -Z_w I_2\left(-\frac{\ell}{2}\right) \quad (36)$$

$$V_3\left(\frac{\ell}{2}\right) = Z_w I_3\left(\frac{\ell}{2}\right) \quad (37)$$

$$V_4\left(-\frac{\ell}{2}\right) = -Z_w I_4\left(-\frac{\ell}{2}\right) \quad (38)$$

$$V_1(0) + j\omega L^{down} I_1(0) = V_2(0) - j\omega L^{down} I_2(0) \quad (39)$$

$$V_3(0) + j\omega L^{up} I_3(0) = V_4(0) - j\omega L^{up} I_4(0) \quad (40)$$

$$-I_1(0) + I_2(0) - I_3(0) + I_4(0) = j\omega C_G [V_1(0) + j\omega L^{down} I_1(0)] \quad (41)$$

$$I_4(0) - I_3(0) = j\omega C_c [V_3(0) + j\omega L^{up} I_3(0)] - j\omega C_c [V_1(0) + j\omega L^{down} I_1(0)] \quad (42)$$

The indexes 1–4 in (35)–(42) represent the respective transmission lines in Fig. 2.

4. RESULTS AND COMPARISON WITH HFSS

The model described in the previous sections applied to the study of the effect of an external plane wave illumination on the orthogonal coupled MTL structure. The results are given as the voltage and current along the length of the lines up to a frequency 3 GHz.

The structure under consideration had these specifications:

$$L_x = L_y = 15 \text{ cm}$$

$$\epsilon_r = 2.55$$

$$w_{up} = 3.85 \text{ mm}, \quad w_{down} = 1.925 \text{ mm}$$

$$Z_w = 50 \Omega$$

The incident uniform plane wave is a *TM* wave with an electric field intensity of $\sqrt{2}$ in the y - z plane (H^i directed as the x axis) and its plane of incidence is also coincident with the y - z plane with $\theta_i = 45^\circ$.

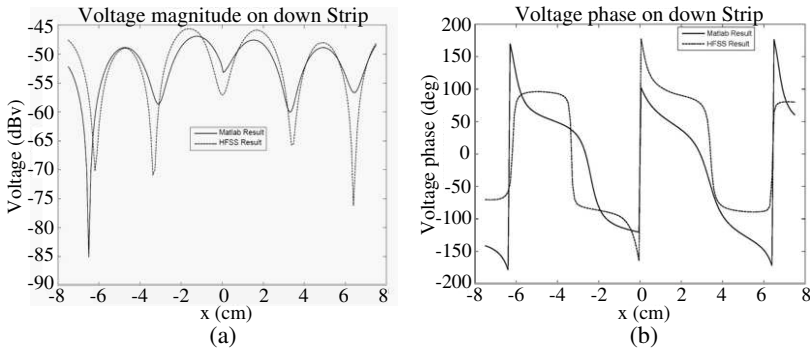


Figure 5. Lower strip voltage from the model in comparison with HFSS: (a) Magnitude, (b) phase.

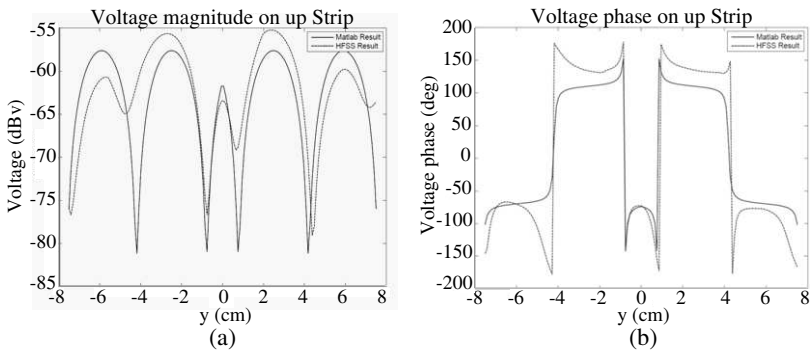


Figure 6. Upper strip voltage from the model in comparison with HFSS: (a) Magnitude, (b) phase.

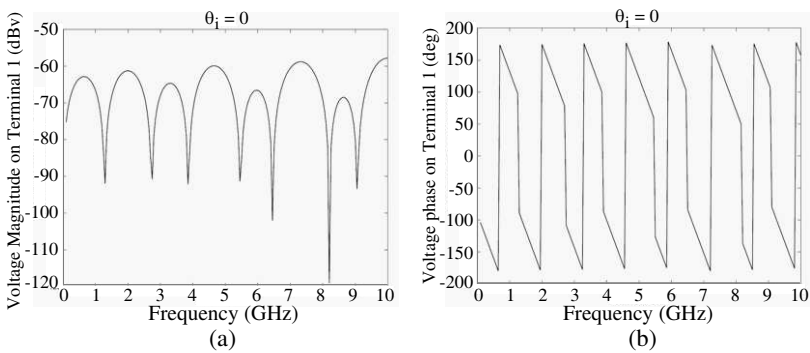


Figure 7. Voltage from the model in Terminal T_1 for a plane of incidence in the z axis: (a) Magnitude, (b) phase.

Fig. 5 shows the magnitude and phase of voltage for the lower strip and Fig. 6 shows those of the upper strip obtained from the proposed model analyzed by MATLAB programming in comparison with the full wave analysis using HFSS along the length of lines.

Figures 5 and 6 show good agreement of the proposed model with the full wave analysis and validate the claim of great precision of this model in practical fabrication experiments. When the plane of incidence is in the z axis and the electric field with intensity of $\sqrt{2}$ is coincident with the bisector of x - y plane, there is a special excitation. Figs. 7 and 8 show the voltage and current in the terminal port of the lower strip (T_1) obtained from the model up to 10 GHz respectively.

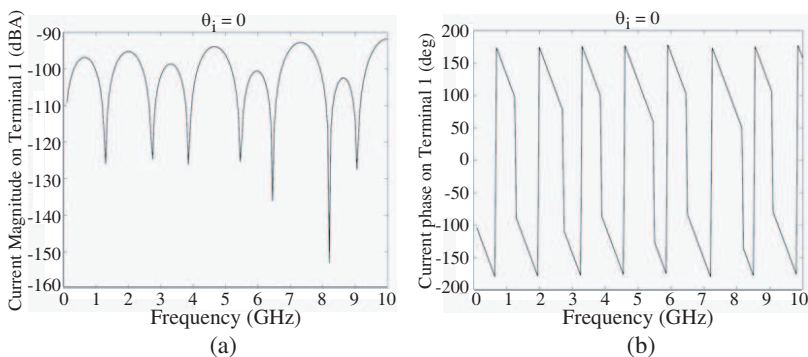


Figure 8. Current from the model in Terminal T_1 for a plane of incidence in the z axis: (a) Magnitude, (b) phase.

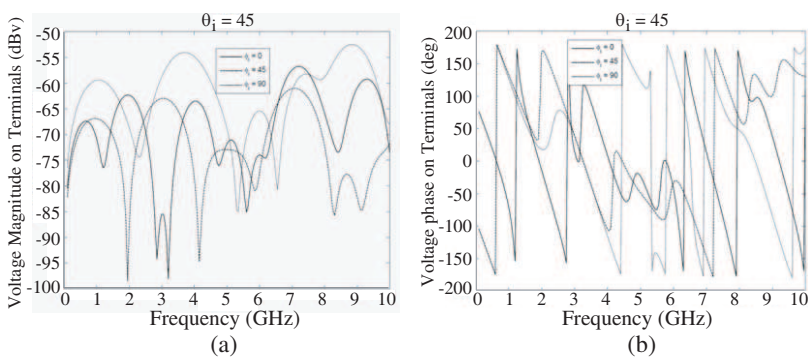


Figure 9. Voltage from the model in terminal T_1 for $\theta_i = 45^\circ$: (a) Magnitude, (b) phase.

Finally voltage and current in the terminal port of the lower strip (T_1) obtained when $\theta_i = 45^\circ$ and electric field intensity is 1 V/m were found. Figs. 9 and 10 show these voltages and currents up to 10 GHz, respectively, when ϕ_i equals to 0° , 45° and 90° . ϕ_i is the angle between \vec{K}_t and x axis.

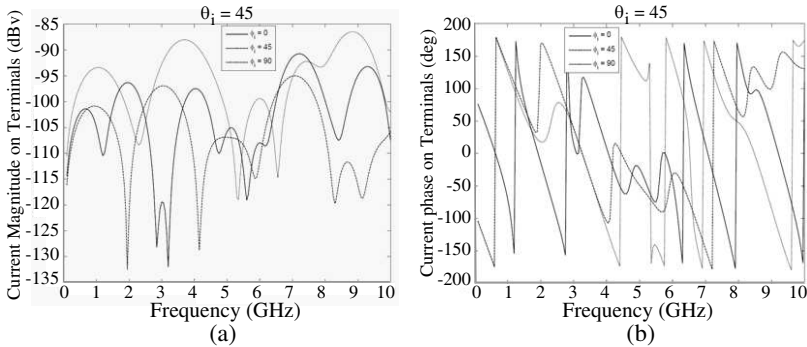


Figure 10. Current from the model in terminal T_1 for $\theta_i = 45^\circ$: (a) Magnitude, (b) phase.

5. CONCLUSION

In this paper, a simple model is presented to analyze crossed orthogonal microstrip lines excited by a uniform plane wave. This structure is simulated using the model of a MTL radiated by an external plane wave and a lumped model of the cross region.

It is shown that this model has a good agreement up to 7 GHz compared to HFSS. Full wave analysis of such a complicated structure with HFSS or CST is time consuming and needs huge processing systems. For example, analysis using the proposed model and MATLAB takes a few seconds but HFSS reaches a convergent solution in more than an hour.

This model can be used to model more complicated structures like crossed orthogonal coupled EMTL (Edged MTL) and multilayer coupled structures. It is shown that the proposed model can be used to design two layer crossed orthogonal microstrip lines with a good accuracy.

REFERENCES

1. Bernardi, P., "Response of a planar microstrip line excited by an electromagnetic field," *IEEE Transaction on Electromagnetic Compatibility*, Vol. 32, No. 2, May 1990.
2. Arshadi, A. and A. Cheldavi, "A simple and novel model for edged microstrip line (EMTL)," *Progress In Electromagnetics Research*, PIER 65, 233–259, 2006.
3. Cheldavi, A. and A. Arshadi, "A simple model for the orthogonal coupled strip lines in multilayer PCB: (Quasi-TEM approach)," *Progress In Electromagnetics Research*, PIER 59, 39–50, 2006.
4. Hashemi-Nasab, M. and A. Cheldavi, "Coupling model for the two orthogonal microstrip lines in two layer PCB board (quasi-TEM approach)," *Progress In Electromagnetics Research*, PIER 60, 153–163, 2006.
5. Khalaj-Amirhosseini, M. and A. Cheldavi, "Optimum design of microstrip RF interconnections," *Journal of Electromagnetic Waves and Applications*, Vol. 18, No. 12, 1707–1715, 2004.
6. Khalaj-Amirhosseini, M. and A. Cheldavi, "Efficient interconnect design using grounded lines," *Journal of Electromagnetic Waves and Applications*, Vol. 17, No. 9, 1289–1300, 2003.
7. Zhengogrg, T., F. Charles, and B. Peter, "Design of multilayer microwave coupled-line structures using thick-film technology," University of Surrey Guildford.
8. Matsanaga, M., M. Katayama, and K. Yasumoto, "Coupled mode analysis of line parameters of coupled microstrip lines," *Progress In Electromagnetic Research*, PIER 24, 1–17, 1999.
9. Homentcovschi, D. and R. Oprea, "Analytically determined quasistatic parameters of shielded or open multiconductor microstrip lines," *IEEE Trans. on Microwave Theory and Techniques*, Vol. 46, No. 1, 18–24, Jan. 1998.
10. Owens, D., "Accurate analytical determination of quasi-static microstrip line parameters," *Radio and Electronic Engineer.*, Vol. 46, No. 7, 360–364, Jul. 1976.
11. Veit, W., H. Diestel, and R. Pregla, "Coupling of crossed planar multiconductor systems," *IEEE Trans. on Microwave Theory and Techniques*, Vol. 30, No. 3, Mar. 1990.
12. Pan, G.-W., K. S. Olson, and B. K. Gilbert, "Frequency-domain solution for coupled striplines with crossing strips," *IEEE Trans. on Microwave Theory and Techniques*, Vol. 39, No. 6, Jun. 1991.
13. Getsinger, W., "Microstrip dispersion model," *IEEE Trans. on*

- Microwave Theory and Techniques*, Vol. 21, 34–39, Jan. 1973.
14. Owens, R. P., “Predicted frequency dependence of microstrip characteristic impedance using the planar waveguide model,” *Electron. Lett.*, Vol. 12, 269–270, 1976.
 15. Edwards, T., *Foundation for Microstrip Design*, Engalco, Knaresborough, UK, 1991.
 16. Pozar, D. M., *Microwave Engineering*, Addison-Wesley Publishing Company, 1990.
 17. Balanis, C. A., *Advanced Engineering Electromagnetics*, John Wiley & Sons, 1989.
 18. Collin, R. E., *Foundation for Microwave Engineering*, McGraw-Hill, 1992.
 19. Heer and C. Love, “Exact inductance equation for conductors with application to non-complicated geometries,” *J. Research National Bureau of Standards-C, Engineering Instrumentation*, Vol. 69C, 127–137, 1965.
 20. Taha, T. E. and M. Elkordy, “Study of biasing effects on coupled microstrip lines characteristics,” *International Symposium on Communications and Information Technologies, ISCIT’06*, 906–909, Sep. 2006.
 21. Fu, J.-H., Q. Wu, Y.-M. Qin, X.-M. Gu, and J.-C. Lee, “Quasi-static parameter analysis for arbitrary metallization thickness of RF MEMS coupled microstrip lines,” *IEEE Antennas and Propagation Society International Symposium*, Vol. 2B, 408–411, Jul. 2005.
 22. Sun, S. and L. Zhu, “Guided-wave characteristics of periodically nonuniform coupled microstrip lines-even and odd modes,” *IEEE Trans. on Microwave Theory and Techniques*, Vol. 53, 1221–1227, Apr. 2005.
 23. Muthana, P. and H. Kroger, “Behavior of short pulses on tightly coupled microstrip lines and reduction of crosstalk by using overlying dielectric,” *IEEE Transactions on Advanced Packaging*, Vol. 30, 511–520, Aug. 2007.
 24. Mehdipour, A. and M. Kamarei, “Fast analysis of external field coupling to orthogonal interconnections in high-speed multilayer MMICs,” *IEEE Transactions on Electromagnetic Compatibility*, Vol. 49, 927–931, Nov. 2007.
 25. Abegaonkar, M. P., H. Yu-Kang, and C. Young-Ki, “Field configurations for electromagnetically (EM) coupled microstrip patch antenna,” *IEEE Antennas and Propagation Society International Symposium*, Vol. 3, 128–131, Jun. 22–27, 2003.

26. Tanaka, T., M. Ueyama, and M. Aikawa, "A push-push oscillator using coupled microstrip lines in common feedback loop," *Microwave Conference, KJMW 2007, Korea-Japan*, 137–140, Nov. 15–16, 2007.
27. Marimuthu, J. and M. Esa, "Wideband and harmonic suppression method of Parallel Coupled Microstrip Bandpass Filter using centered single groove," *IEEE International Conference on Telecommunications and Malaysia International Conference on Communications*, 622–626, May 14–17, 2007.
28. Filho, P. N. S., A. L. Bezzera, A. J. B. De Oliveira, and M. T. De Melo, "Frequency shifting using corrugated coupled microstrip lines," *IEEE MTT-S International Conference*, 47–50, Jul. 2005.
29. Enokihara, A., H. Yajima, M. Kosaki, H. Murata, and Y. Okamura, "Guided-wave electro-optic modulator using resonator electrode of coupled microstrip lines," *Electron. Lett.*, Vol. 39, 1671–1673, Nov. 2003.
30. Enokihara, A., H. Furuya, H. Yajima, M. Kosaki, H. Murata, and Y. Okamura, "60 GHz guided-wave electro-optic modulator using novel electrode structure of coupled microstrip line resonator," *International Microwave Symposium, 2004 IEEE MTT-S*, Vol. 3, 2055–2058, Jun. 6–11, 2004.
31. Subbiah, S. and A. Alphones, "Tunable isolator using a coupled microstrip line with an obliquely magnetised YIG substrate," *IEE Proceedings — Microwaves, Antennas and Propagation*, Vol. 150, 219–222, Aug. 2003.
32. Rahim, M. K. A., Z. W. Low, P. J. Soh, A. Asrokin, M. H. Jamaluddin, and T. Masri, "Aperture coupled microstrip antenna with different feed sizes and aperture positions," *International RF and Microwave Conference*, 31–35, Sept. 12–14, 2006.
33. Saksiri, W. and M. Krairiksh, "Lumped element model approach for the bandwidth enhancement of coupled microstrip antenna," *Proceedings of the 2003 International Symposium on Circuits and Systems*, Vol. 1, 581–584, May 25–28, 2003.
34. Nickel, J. G. and J. E. Schutt-Aine, "Matched coupled microstrip transistor amplifier methodology," *IEEE Transactions on Advanced Packaging*, Vol. 26, 361–367, Nov. 2003.
35. Qinjiang, R. and R. H. Johnston, "Modified aperture coupled microstrip antenna," *IEEE Transactions on Antennas and Propagation*, Vol. 52, 3397–3401, Dec. 2004.
36. Shih, C.-H., G.-H. Shiue, T.-L. Wu, and R.-B. Wu, "The

- effects on SI and EMI for differential coupled microstrip lines over LPC-EBG power/ground planes,” *Asia-Pacific Symposium on Electromagnetic Compatibility and 19th International Zurich Symposium on Electromagnetic Compatibility*, 164–167, May 19–23, 2008.
37. Pan, Z. H. and J. H. Wang, “Design of the UWB bandpass filter by coupled microstrip lines with U-shaped defected ground structure,” *International Conference on Microwave and Millimeter Wave Technology*, Vol. 1, 329–332, Apr. 21–24, 2008.
 38. Sharma, A. K., R. Singh, and A. Mittal, “Wide band dual circularly polarized aperture coupled microstrip patch antenna with bow tie shaped apertures,” *International IEEE Symposium on Antennas and Propagation*, Vol. 4, 3749–3752, Jun. 20–25, 2004.